International Journal of Pharmaceutics: X 4 (2022) 100141

Contents lists available at ScienceDirect

International Journal of Pharmaceutics: X

journal homepage: www.sciencedirect.com/journal/international-journal-of-pharmaceutics-x

Long term behavior of dexamethasone-loaded cochlear implants: In vitro & in vivo

T. Rongthong [a,1], A. Qnouch [a,1], M. Maue Gehrke [a], F. Danede [b], J.F. Willart [b], P.F.M. de Oliveira [b], L. Paccou [b], G. Tourrel [c], P. Stahl [c], J. Verin [a], P. Toulemonde [a], C. Vincent [a], F. Siepmann [a], J. Siepmann [a,*]

[a] Univ. Lille, Inserm, CHU Lille, U1008, F-59000 Lille, France
[b] Univ. Lille, UMR CNRS 8207, UMET, F-59655 Villeneuve d'Ascq, France
[c] Oticon Medical, R&D, 06224 Vallauris, France

ARTICLE INFO

Keywords:
Cochlear implant
Dexamethasone
Silicone
Raman imaging
Diffusion

ABSTRACT

The aim of this study was to better understand the long term behavior of silicone-based cochlear implants loaded with dexamethasone: in vitro as well as in vivo (gerbils). This type of local controlled drug delivery systems offers an interesting potential for the treatment of hearing loss. Because very long release periods are targeted (several years/decades), product optimization is highly challenging. Up to now, only little is known on the *long term* behavior of these systems, including their drug release patterns as well as potential swelling or shrinking upon exposure to aqueous media or living tissue. Different types of cylindrical, cochlear implants were prepared by injection molding, varying their dimensions (being suitable for use in humans or gerbils) and initial drug loading (0, 1 or 10%). Dexamethasone release was monitored in vitro upon exposure to artificial perilymph at 37 °C for >3 years. Optical microscopy, X-ray diffraction and Raman imaging were used to characterize the implants before and after exposure to the release medium in vitro, as well as after 2 years implantation in gerbils. Importantly, in all cases dexamethasone release was reliably controlled during the observation periods. Diffusional mass transport and limited drug solubility effects *within* the silicone matrices seem to play a major role. Initially, the dexamethasone is homogeneously distributed throughout the polymeric matrices in the form of tiny crystals. Upon exposure to aqueous media or living tissue, limited amounts of water penetrate into the implant, dissolve the drug, which subsequently diffuses out. Surface-near regions are depleted first, resulting in an increase in the apparent drug diffusivity with time. No evidence for noteworthy implant swelling or shrinkage was observed in vitro, nor in vivo. A simplified mathematical model can be used to facilitate drug product optimization, allowing the prediction of the resulting drug release rates during decades as a function of the implant's design.

1. Introduction

Up to date, there is an unmet need for reliable drug delivery to the inner ear (the cochlea) (El Kechai et al., 2015; Chin and Diaz, 2019; Hao and Li, 2019; Lehner et al., 2021; Maeder et al., 2018). This is due to the blood-cochlear-barrier, which effectively hinders the transport of drugs from the blood stream to the target site (Swan et al., 2008), similar to the protection of the brain by the blood-brain-barrier. Direct drug administration into the inner ear can overcome this obstacle, but is highly invasive. In clinical practice, repeated injections are not feasible, due to the risk of infections and damage of this highly sensitive organ. Also, the volume of the liquid in the inner ear is very limited.

The World Health Organization (WHO) warns that about 2.5 billion people will be living with some degree of hearing loss by 2050: approximately 25% of the world's population (World Health Organization, 2021). The consequences of hearing loss can be severe and affect all ages (Olusanya et al., 2014; Nordvik et al., 2018). For example, language development and education can be impacted for children. Elderly often suffer from the resulting social isolation and loneliness, and might not be able to live independently anymore. Overall, the

* Correspondimg author at: University of Lille, College of Pharmacy, INSERM U1008, 3 rue du Professeur Laguesse, 59006 Lille, France.
E-mail address: juergen.siepmann@univ-lille.fr (J. Siepmann).
[1] *Contributed equally*

https://doi.org/10.1016/j.ijpx.2022.100141
Received 23 September 2022; Received in revised form 17 November 2022; Accepted 19 November 2022
Available online 22 November 2022

quality of life and well-being of the person can be tremendously affected.

For patients suffering from severe hearing loss, the implantation of metal electrodes into the inner ear was shown to provide a potential treatment (most commonly the noble metal platinum is used for this purpose). The concept is to bypass the pathological inner ear that is not able to convey acoustic environmental sounds anymore. Those sounds are rather translated into electrical signals that directly stimulate the auditory nerve. Each electrode contact is being placed at a different cochlear location with the expectation that the ensemble excites auditory fibers at frequencies following the tonotopical logic. For that, the electrodes are connected to the main implant body by insulated wires (separated by silicone). This cochlear implant element, inserted inside the cochlea and composed of electrode contacts, wires and silicon, is also called "electrode array". Since many years, this type of intracochlear implants is used in clinical practice to treat patients suffering from profound to severe hearing loss. However, the placement of the miniaturized implants is invasive and potentially causes trauma and the death of remaining "hair cells" or of neighboring neural elements playing a key role for the hearing process. Furthermore, fibrosis can be induced (the implants being foreign bodies), which in turn can decrease the efficacy of the electrical transmissions in the inner ear and, thus, the performance of the hearing aid.

To overcome these drawbacks, the local release of low amounts of dexamethasone over prolonged periods of time has been proposed (Astolfi et al., 2016; Bas et al., 2016; Douchement et al., 2015; Qnouch et al., 2021). Several beneficial effects of such a glucocorticoid treatment can be expected: (i) The importance of inflammation caused by implant placement can be reduced, (ii) fibrosis be limited, and (iii) the life-time expectancy of remaining hair cells be increased (Jia et al., 2016; Liu et al., 2015; Gao et al., 2021; Toulemonde et al., 2021). One possible strategy is to incorporate dexamethasone into the silicone matrices separating the metal electrodes in the cochlear implants (Farahmand Ghavi et al., 2010; Krenzlin et al., 2012; Farhadi et al., 2013; Liu et al., 2016). The idea is to trap the drug in the polymeric matrix to avoid immediate release and to be able to control the release rate of the corticoid during several years. Interestingly, dexamethasone-loaded silicone matrices have also been used for a different clinical application: in pacemakers. In that case, the aim is to continuously release small amounts of this corticoid from silicone rings located in the vicinity of the pacemaker electrodes in order to minimize fibrosis and, thus, to keep the simulation threshold values low. Importantly, this type of system proved to be clinically effective for at least 10 years (Mond and Stokes, 1996). Silicone matrices are also used for other types of local controlled drug delivery systems, e.g. vaginal rings (McCoy et al., 2021) and intravesical devices (Palugan et al., 2021).

Alternative local drug delivery strategies for inner ear treatments include biodegradable intracochlear implants (Lehner et al., 2019; Lehner et al., 2022), semi-solid dosage forms administered into the *middle* ear (Borden et al., 2011; Gausterer et al., 2020; El Kechai et al., 2016; Engleder et al., 2014), micropumps (Forouzandeh et al., 2019), microneedles (Aksit et al., 2021) and nanoparticles (Jaudoin et al., 2021a; Dai et al., 2018). For example, an interesting recent study reported on dexamethasone-loaded implants based on poly(lactic-*co*-glycolic acid) (PLGA) (Lehner et al., 2019). The systems were prepared by hot melt extrusion. Polyethylene glycol (PEG) was added to provide desired mechanical implant properties, in particular flexibility. In case a drug delivery system is not directly administered into the cochlea, but into the middle ear, upon release the drug has to subsequently enter the cochlea, e.g. via diffusion through the round or oval window in order to reach its target side. The use of liposomes has been reported to potentially help controlling drug release as well as the transport into the inner ear (Jaudoin et al., 2021b).

Different types of physico-chemical phenomena can be involved in the control of drug release from polymeric matrices, including diffusional mass transport (e.g., of water and dissolved drug molecules) (Crank, 1975), the dissolution of drug particles (Siepmann and Siepmann, 2013), polymer swelling, degradation and/or dissolution (Lao et al., 2008), limited drug solubility effects in the surrounding fluid and/or *within* the delivery system (Siepmann and Siepmann, 2020), pore formation, osmotic effects and drug-polymer interactions, to mention just a few. Mathematical theories describing these processes in a quantitative and mechanistically realistic manner can be very helpful to better understand how the devices work (Borgquist et al., 2006). Ideally, such theories allow to predict the effects of the design of this type of advanced delivery systems on the resulting drug release kinetics, facilitating device optimization. This should not be confused with *empirical* mathematical models, which can generally not help elucidating the underlying drug release mechanisms (being purely descriptive). Furthermore, appropriate *experimental* analytical techniques can be very helpful to better understand how a drug is released from a dosage form (Bawuah and Zeitler, 2021; Zeitler et al., 2007; Punčochová et al., 2016). In particular, imaging techniques (such as Raman mapping) can provide very interesting information on time-dependent changes in the location of the drug in the drug delivery system and potential alterations of the inner structure of the device during drug release. For instance, crack formation in polymeric film coatings surrounding drug-loaded cores might be evidenced (Vukosavljevic et al., 2016).

The aim of this study was to better understand the long term behavior of dexamethasone-loaded cochlear implants (free of metal electrodes) in vitro and in vivo. Different types of systems were prepared, with dimensions allowing for administration to humans and gerbils. The implants were prepared by injection molding, the initial drug loading was varied from 0 to 10%. Optical microscopy, X-ray diffraction and Raman imaging were used to characterize the implants before and after exposure to artificial perilymph in vitro and placement into gerbils in vivo. In vitro drug release and potential device swelling/shrinking was monitored for >3 years. The in vivo study was conducted for 2 years.

2. Materials and methods

2.1. Materials

Kits for the preparation of silicone elastomers (MED-4735; NuSil Technology, Carpinteria, USA); dexamethasone (polymorphic Form A; Discovery Fine Chemicals, Dorset, UK); calcium chloride dihydrate, magnesium sulfate tetrahydrate, potassium chloride, sodium chloride and 4-(2-hydroxyethyl) piperazine-1-ethanesulfonic acid (HEPES) (HEPES Pufferan; Carl Roth, Lauterbourg, France); acetonitrile (HPLC grade; Fisher Scientific, Illkirch, France); MilliQ water (obtained with a Millipore Integral 5 apparatus; Millipore Corporation, Billerica, USA).

2.2. Preparation of cochlear implants

Equal amounts of MED-4735 Parts A and B (approximately 5 g each) were passed separately 10 times through a two-roll mill (Chef Premier KMC 560/AT970A; Kenwood, Havant, UK). To initiate polymer cross-linking, both parts were manually blended and the mixture was passed 10 times through the mill. Subsequently, appropriate amounts of dexamethasone powder (as received) were added (except for drug-free implants), and the mixture was passed another 40 times through the mill. The obtained mass was injected into stainless-steel molds (Oticon Medical, Lyngby, Denmark) to shape the silicon mass into cochlear implants. The implant dimensions were suitable for use either in humans (Krenzlin et al., 2012) or in gerbils (length: 3 mm, diameter: 0.2 mm). The molds were placed under a hydraulic press at 4.5 bars and heated to 110 °C for 10 min to complete cross-linking. Ethanol (96% *v*/v) was injected into the molds in order to remove the implants.

2.3. Optical microscopy

The inner and outer morphology of the cochlear implants was monitored using a Nikon Eclipse SMZ-U microscope, equipped with an

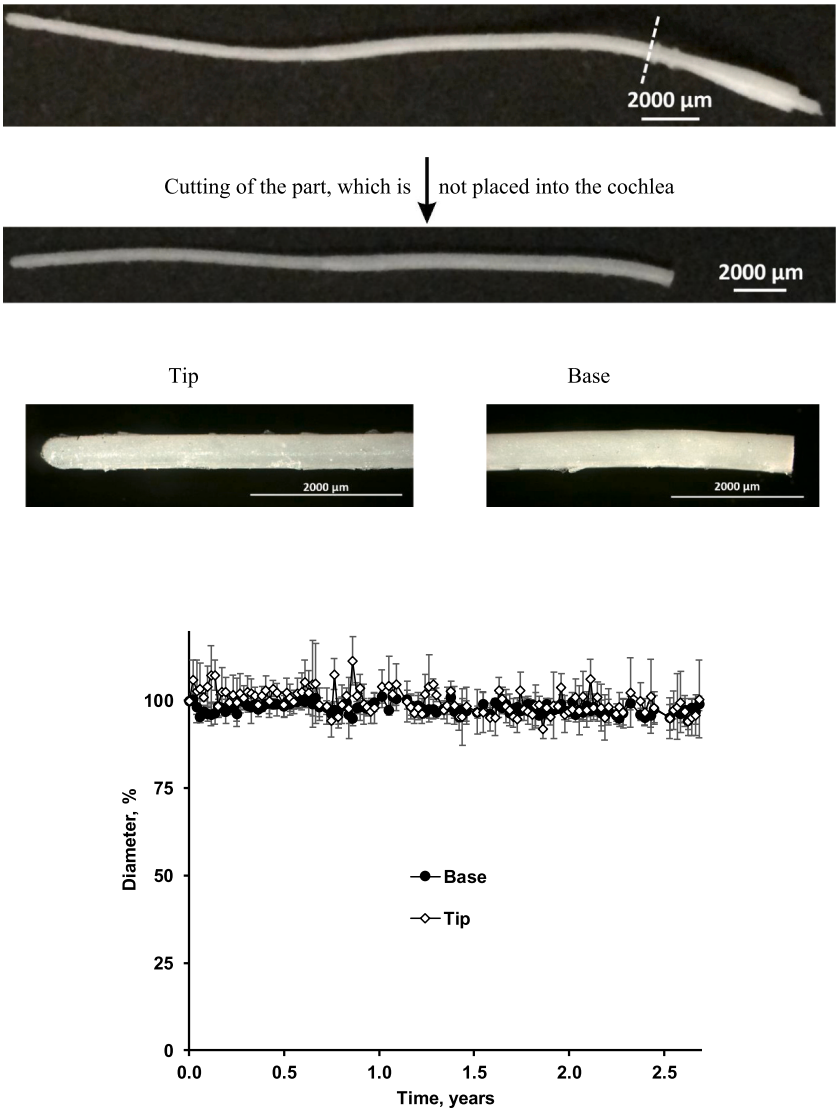

Fig. 1. *Top:* Optical microscopy pictures of a cochlear implant for use in humans (without metal electrodes), loaded with 10% dexamethasone (after manufacturing). For the drug release and swelling studies, the part of the implant, which is not placed into the cochlea, was cut off (at the dashed line). *Bottom:* Dynamic changes in the diameters of the "tips" and "bases" of the implants upon long term exposure to artificial perilymph at 37 °C (in vitro) ($n = 4$, mean values +/− standard deviations).

AxioCam ICc 1 Zeiss camera (Zeiss, Oberkochen, Germany). Cross-sections were obtained using a cryostat.

2.4. X-ray diffraction

A Panalytical X'pert Pro diffractometer (PANalytical, Almelo, Netherlands) in transmission mode with an incident beam parabolic mirror (λ Cu, Kα = 1.54 Å) was used to record X-ray diffraction patterns. The samples were placed inside Lindemann glass capillaries (diameter 1 mm; Hilgenberg, Malsfeld, Germany), which were fixed on a spinning sample holder.

2.5. Drug release measurements

Implants for humans were cut as illustrated at the top of Fig. 1 to remove the parts, which are not inserted into the cochlea. Samples were placed into 2 mL HPLC glass vials (1 implant per vial; screw-top amber glass; Sigma Aldrich, St. Quentin Fallavier, France), containing 0.2 mL inserts and 70 µL artificial perilymph: an aqueous solution of 1.2 mmol calcium chloride dihydrate, 2 mmol magnesium sulfate tetrahydrate, 2.7 mmol potassium chloride, 145 mmol sodium chloride and 5 mmol HEPES Pufferan. The vials were horizontally shaken at 80 rpm and 37 °C (GFL 3033; Gesellschaft fuer Labortechnik, Burgwedel, Germany). At predetermined time points, the release medium was completely renewed. The drug concentration in the withdrawn samples was determined by HPLC analysis using an Alliance e2695 apparatus (Waters Division, Milford, USA), equipped with an UV detector. Samples (50 µL) were injected into a reverse phase column C18 (Gemini 3 µm, 110 Å, 100 × 4.6 mm, Phenomenex, Le Pecq, France) (mobile phase = acetonitrile:water 33:67 V:V, flow rate = 1.2 mL/min). Dexamethasone was detected at λ = 220 nm.

Each experiment was performed 4 times, mean values +/− standard deviations are reported.

2.6. Monitoring of implant swelling

Implants for humans were treated as for the in vitro drug release measurements described in *Section 2.5. Drug release measurements*. Dynamic changes in the diameters of the "tips" and "bases" of the systems (Fig. 1) were monitored using a Nikon Eclipse SMZ-U microscope, equipped with an AxioCam ICc 1 Zeiss camera (Zeiss, Oberkochen, Germany). At predetermined time points, samples were withdrawn and analyzed. Each experiment was performed 4 times, mean values +/− standard deviations are reported.

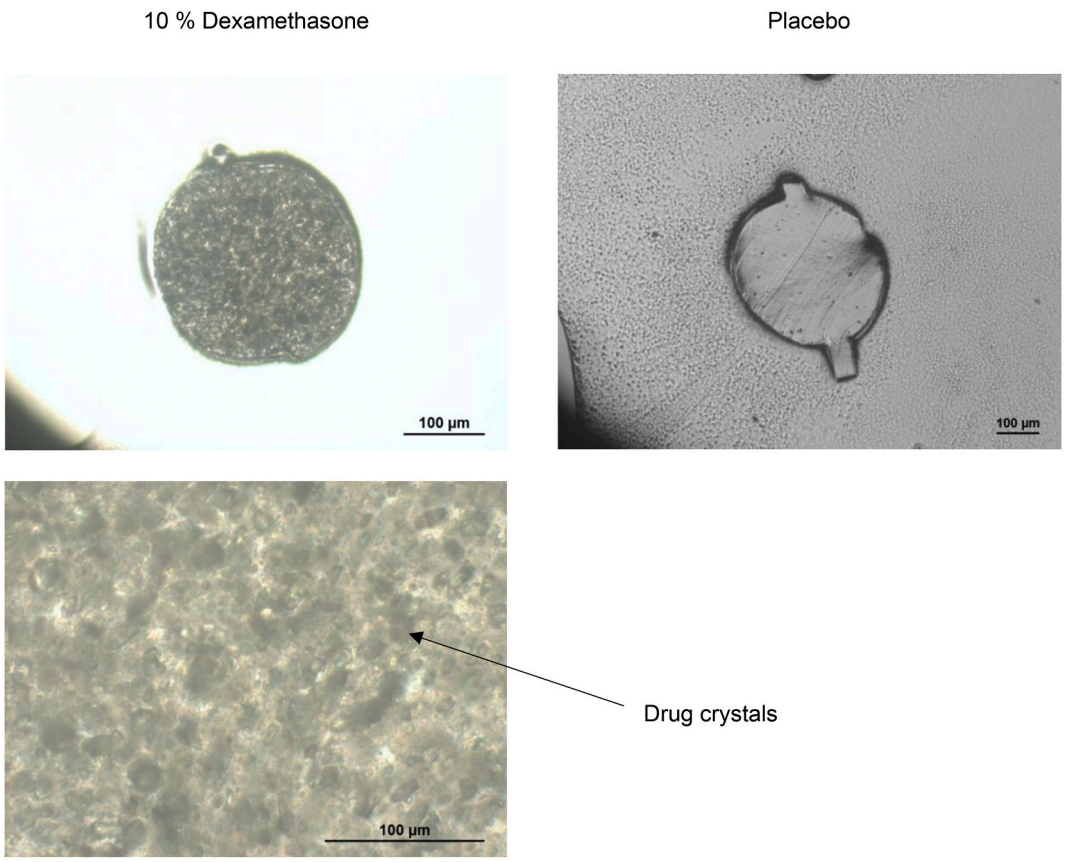

Fig. 2. Optical microscopy pictures of radial cross-sections of cochlear implants for humans (without metal wires & electrodes) after manufacturing: Loaded with 10% dexamethasone (left hand side) or free of drug (placebo, right hand side).

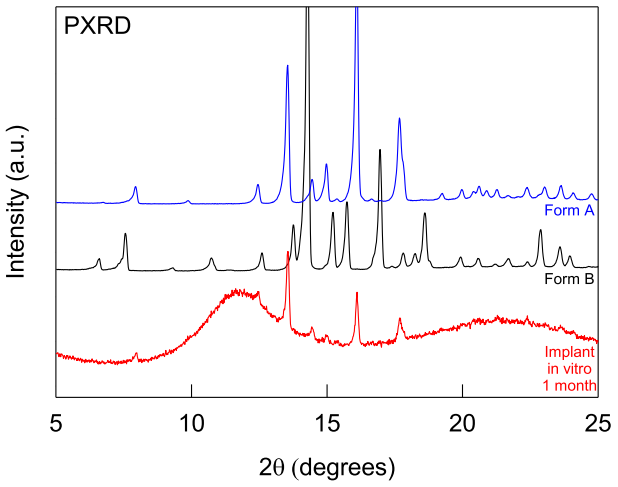

Fig. 3. X-ray diffraction patterns of cochlear implants for humans loaded with 10% dexamethasone after 1 month exposure to artificial perilymph at 37 °C (in vitro). For reasons of comparison, also the X-ray diffraction patterns of the 2 known polymorphic forms of dexamethasone are shown.

2.7. Raman imaging

Implants were analyzed using a Renishaw InVia Raman spectrometer, coupled to a Leica microscope. The 785 nm line emitted from a Renishaw laser diode was focused via a x50 long working distance Leica objective. Under these conditions, ~200 μm^3 volumes were analyzed within the samples at each XY position. The spectral resolution was about 2 cm^{-1} in the investigated spectral window (500–1000 cm^{-1}). Raman mapping was performed by scanning 100 × 100 μm^2 up to 500 × 500 μm^2 areas, using the classical sequential (point by point) method (from 1 µm up to 5 µm between points). During Raman mapping, 600 up to 10,000 spectra were collected with an acquisition time ranging between 1 s up to 3 s. Raman images were calculated using the DCLS (Direct Classical Least Square) method, fitting each spectrum to a linear combination of Raman spectra of the sample components.

2.8. In vivo study

Cochlear implants (initially drug-free, or loaded with 1 or 10% dexamethasone, $n = 6$ for each group) were inserted into the inner ears of Mongolian gerbils. The systems were explanted after 2 years, cut with a cryostat and analyzed by Raman imaging. The work was conducted in agreement with the standard guidelines of the French Ministry of Agriculture, according to the EU Directive 2010/63/EU for the protection of animals used for scientific purposes. The study was approved by the regional committee for experimental animal care and use (CEEA Nord-Pas de Calais n°75, Lille, France; protocol # 2017071021362273). The surgical procedure was performed under general anesthesia using a Minitag veterinary gas anesthesia station (Tem Sega, Pessac, France). A mixture of air (2 L/min) and isoflurane (5%) was used for induction, and maintenance was achieved with 0.8 L/min of air and 1.5–2% isoflurane (Aerrane; Baxter, Deerfiel, IL, USA). An injection of buprenorphine (Bupaq 0.3 mg/mL; Virbac, Carros, Carros, France) at a dosage of 0.1 mg/kg was performed 45 min before the incision. Lidocaine (Xylocaine spray 5%; Astrazeneca, London, UK) was used at the incision site to optimize local pain control. All procedures were performed by the same operator after a period of training of a few months. A small right retroauricular incision was made and the muscles covering the bulla were

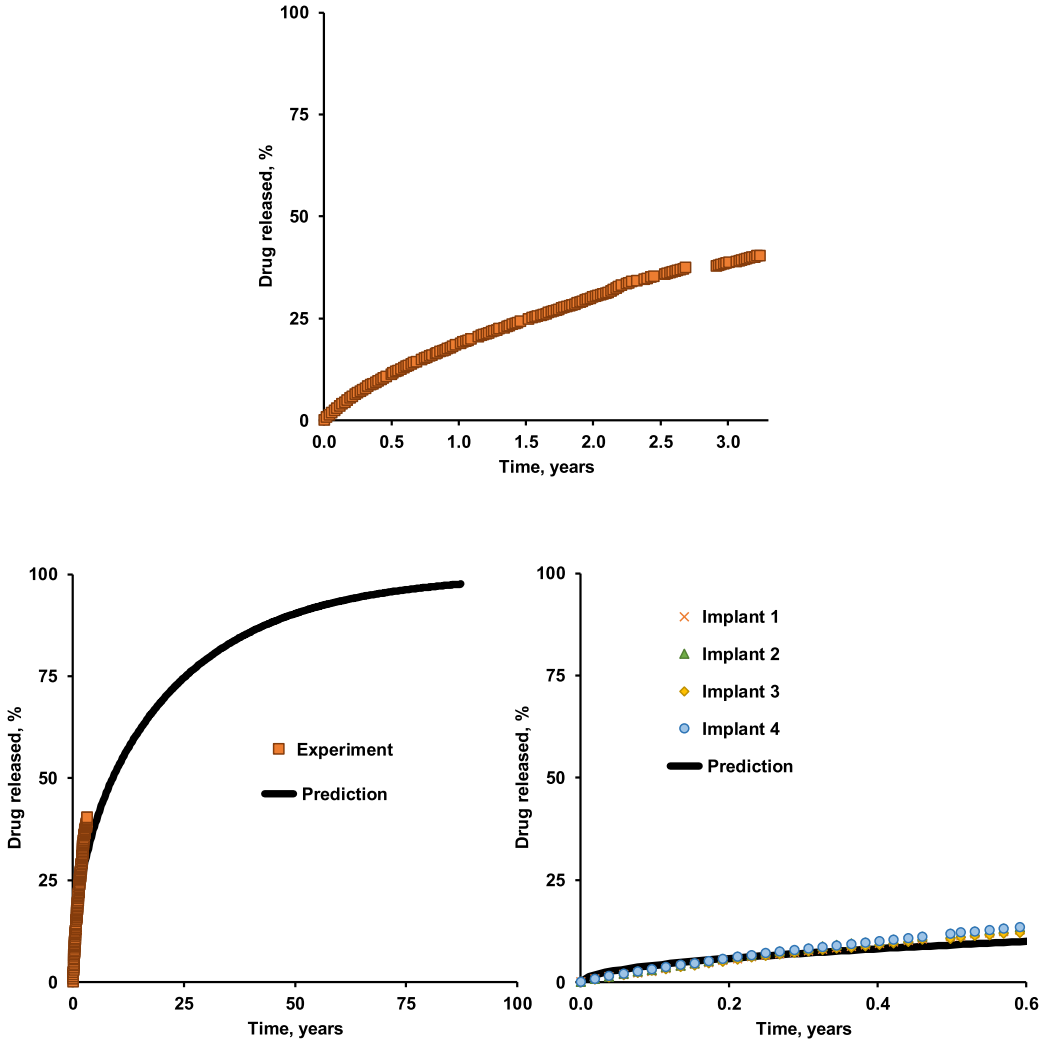

Fig. 4. In vitro drug release from cochlear implants for humans (without metal wires & electrodes) loaded with 10% dexamethasone in artificial perilymph at 37 °C. The upper diagram shows the experimentally measured values (n = 4, error bars are too small to be visible). The diagrams at the bottom illustrate in addition the theoretically predicted release profile (calculated using Eq. 1, details are given in the text). The diagram on the right hand side shows the release profiles from 4 individual implants during the first 7 months.

retracted. The anterior portion (anterior to the upper pillar) of the bulla was opened with micro forceps to expose the round window, which was then clearly visible. The window was opened and the implant was carefully inserted. An inert, immediately curing silicone (Kwik sil, world precision instrument, Sarasota, FL, USA) was instilled into the auditory bulla to allow the system to be maintained. The incisions were then sutured in a skin plane. After 2 years, the animals were euthanized and the implants collected.

3. Results and discussion

3.1. Physical state and distribution of the drug after manufacturing

The picture at the top of Fig. 1 shows a cochlear implant loaded with 10% dexamethasone for humans after manufacturing. The implant consists of silicone and drug only: no metal electrodes or wires were included. For the dexamethasone release measurements and swelling studies, the part of the implant, which is not inserted into the cochlea (on the right hand side) was cut off (as illustrated at the top of Fig. 1). The images on the left hand side of Fig. 2 show optical microscopy pictures of radial cross-sections of such an implant (at different magnifications). For reasons of comparison, the picture on the right hand side in Fig. 2 shows a radial cross-section through a cochlear implant *free of drug* (placebo). As it can be seen, the latter (consisting of silicone only) was transparent. In contrast, darker regions were visible in the dexamethasone-loaded implant. They likely indicate the presence of drug particles, hindering the visible light to pass through the sample. This is consistent with previously reported Scanning Electron Microscopy pictures of polymeric films and cylindrical extrudates based on the same silicone and drug: Krenzlin et al. (Krenzlin et al., 2012) evidenced the presence of tiny dexamethasone crystals distributed throughout such silicone matrices. Importantly, the drug crystal distribution seems to be homogenous throughout the implant (Fig. 2, left hand side). Similar observations were made with the cochlear implants for use in *gerbils* (which were smaller).

Since two polymorphic forms of dexamethasone have recently been reported (Forms A and B) (Oliveira et al., 2018), it was interesting to know which polymorph was present in the investigated cochlear implants. For this reason, X-ray diffraction patterns of the implants were recorded, as well as of the 2 known polymorphic forms of dexamethasone. As it can be seen in Fig. 3, the diffraction patterns of dexamethasone Form A (the powder used as received in this study, blue curve) and Form B (prepared by milling and heating, as described in (Oliveira et al., 2018), black curve) can be distinguished by several peaks observed at

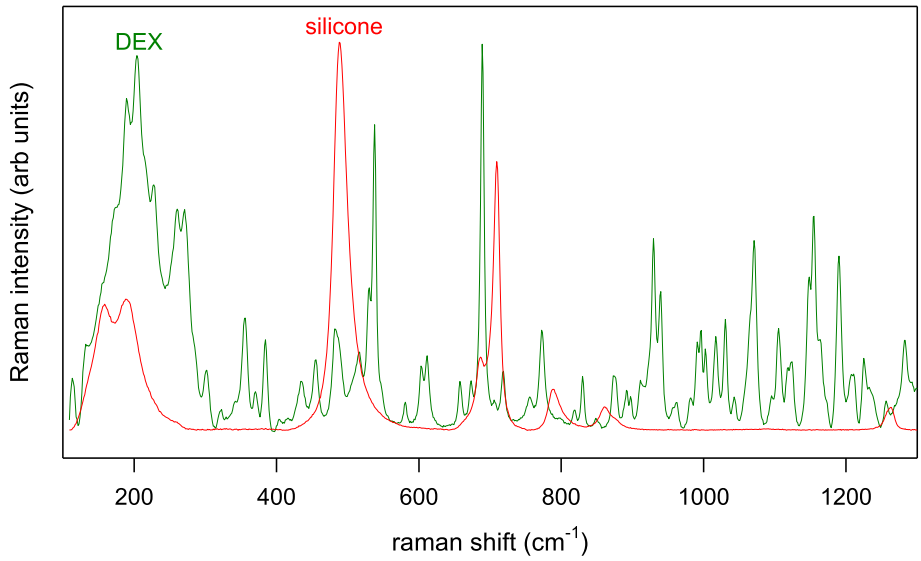

Fig. 5. Raman spectra of the investigated silicone and dexamethasone. Drug-free silicone implants and drug powder (as received) were studied.

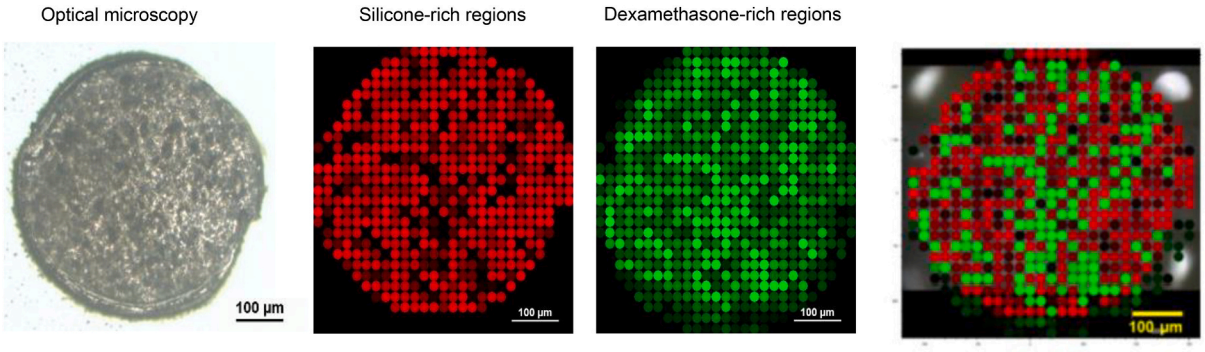

Fig. 6. Optical microscopy picture and Raman images of a radial cross-section of a cochlear implant for humans (without metal electrodes), loaded with 10% dexamethasone *after manufacturing*.

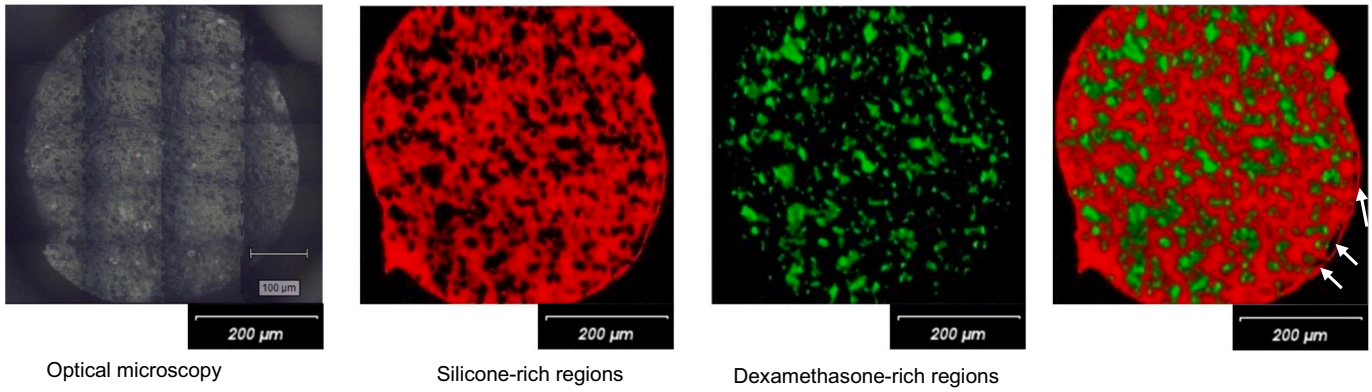

Fig. 7. Optical microscopy picture and Raman images of a radial cross-section of a cochlear implant for humans (without metal electrodes), initially loaded with 10% dexamethasone *after 1 month exposure to artificial perilymph at 37 °C (*in vitro*)*. The white flashes highlight regions which might correspond to dexamethasone-depleted regions.

different angles. Clearly, the diffraction patterns of the drug-loaded implants after 1 month exposure to artificial perilymph (red curve) corresponded to those of dexamethasone Form A. Thus, neither the manufacturing process of the cochlear implants used in this study, nor the exposure to the release medium changed the polymorphic form of the drug.

3.2. Implant swelling and drug release in vitro

From a practical point of view, it is critically important that the cochlear implants do not substantially swell upon contact with aqueous media. Otherwise, the inner ear might be damaged. To monitor potential changes in the dimensions of the investigated implants in vitro, the latter

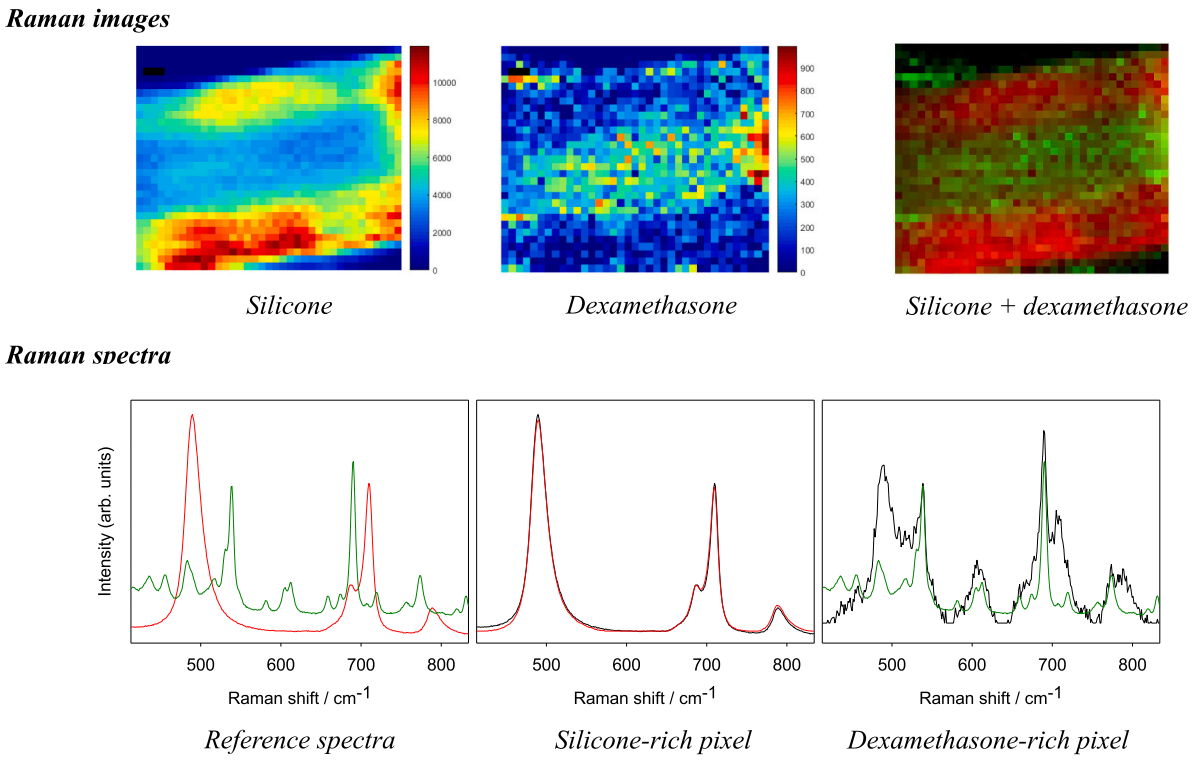

Fig. 8. Raman images (pixel size: 20 × 20 μm) and Raman spectra of a longitudinal cross-section of a cochlear implant, which was explanted from a gerbil after 2 years. The color scales indicate relative silicone or dexamethasone concentrations. In the Raman image on the right hand side, silicone-rich regions are marked in red, and dexamethasone-rich regions in green. (For interpretation of the references to color in this figure legend, the reader is referred to the web version of this article.)

were exposed to artificial perilymph at 37 °C and horizontally shaken at 80 rpm for 3 years. At pre-determined time points, samples were withdrawn and their diameters were measured using a Nikon Eclipse SMZ-U microscope, equipped with an AxioCam ICc 1 Zeiss camera. The pictures in the middle of Fig. 1 show the locations for these measurements: at the "tips" and "bases" of the implants. The diagram at the bottom of Fig. 1 shows the swelling behavior during long term exposure to artificial perilymph. Importantly, no substantial variations in the systems' diameters were observed. The implants did neither swell, nor shrink to a noteworthy extent. The observed arbitrary and limited "fluctuations" can probably be explained as follows: The radial cross-section of an implant was not *perfectly* spherical (see for instance the pictures at the top of Fig. 2). Thus, the *exact position* of the implant during the microscopic observation impacts the measured diameter to a certain degree. This *technical* bias does not reflect real implant swelling/shrinking.

The experimentally measured dexamethasone release kinetics from cochlear implants for humans loaded with 10% drug in artificial perilymph are illustrated in the diagram at the top of Fig. 4. The error bars are too small to be visible. Clearly, drug release is controlled during several years (e.g., about 40% of the initial dexamethasone loading was released after 3.2 years). This is in good agreement with results previously reported on silicone-based cochlear implants of the same composition, but containing also metal wires & electrodes (Krenzlin et al., 2012). Thus, the presence/absence of the metal pieces does not seem to substantially impact the relative drug release rate from these systems. This is consistent with the hypothesis that drug diffusion through the silicone matrix plays a major role in the control of dexamethasone release from this type of advanced drug delivery systems: Upon contact with aqueous fluids, water penetrates into the system and dissolves the drug. Once dissolved, the dexamethasone slowly diffuses out into the surrounding environment. The following equation has been proposed for the quantification of drug release from such electrode-containing implants (assuming cylindrical geometry) (Krenzlin et al., 2012; Crank, 1975):

$$\frac{M_t}{M_\infty} = 1 - \frac{32}{\pi^2} \cdot \sum_{n=1}^{\infty} \frac{1}{q_n^2} \cdot exp\left(-\frac{q_n^2}{R^2} \cdot D \cdot t\right) \cdot \sum_{p=0}^{\infty} \frac{1}{(2 \cdot p + 1)^2} \cdot exp\left(-\frac{(2 \cdot p + 1)^2 \cdot \pi^2}{H^2} \cdot D \cdot t\right) \quad (1)$$

where M_t and M_∞ are the absolute cumulative amounts of drug released at time t and *infinity*, respectively; n and p are a dummy variables; q_n are the roots of the Bessel function of the first kind of zero order [$J_0(q_n) = 0$]; D is the "apparent" diffusion coefficient of dexamethasone within the silicone matrix; R and H denote the radius and height of the cylindrical implants.

This equation can be derived from Fick's second law of diffusion, assuming that: (i) drug diffusion is the dominant mass transport process (e.g. is much faster than drug dissolution and water diffusion), (ii) perfect sink conditions are provided throughout the experiments in the surrounding bulk fluid, (iii) the drug is initially homogeneously distributed throughout the system, (iv) the diffusion coefficient of the drug is not dependent on time or position, (v) the implants are of cylindrical geometry, (vi) drug diffusion occurs in radial and axial direction, (vii) the implant does not dissolve or swell upon exposure to the release medium to a noteworthy extent, and (viii) limited solubility effects *within* the implants are negligible. Please note that the latter assumption is likely not fulfilled in the case of these implants, because the amounts of water available for drug dissolution within the systems are limited. Thus, the term "diffusion coefficient" refers to the "*apparent* diffusion coefficient" of the drug in this study.

Krenzlin et al. (Krenzlin et al., 2012) used Eq. 1 to theoretically predict dexamethasone release from cochlear implants based on the same silicone, loaded with 10–30% drug. But in that study, the implants contained metal electrodes and the release medium was not agitated. The apparent diffusion coefficient of the drug in the polymeric matrix had been estimated by fitting an appropriate solution of Fick's second law of diffusion to experimentally determined dexamethasone release kinetics from thin *films* of the same composition (free of electrodes)

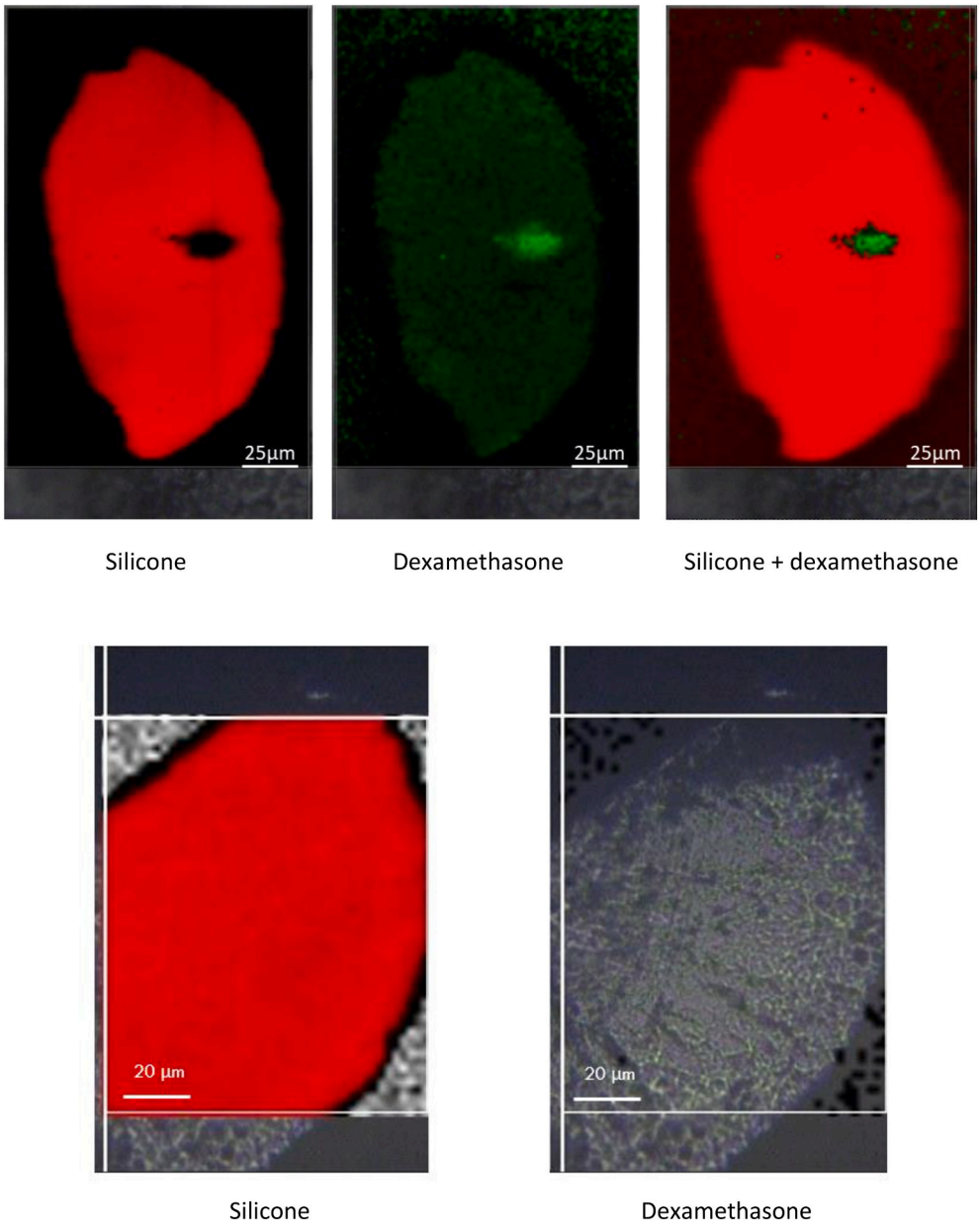

Fig. 9. Raman images of two radial cross-sections of a cochlear implant, which was explanted from a gerbil after 2 years. The pictures at the top correspond to one cross-section, the pictures at the bottom to the other cross-section. The implant was initially loaded with 10% dexamethasone.

(Krenzlin et al., 2012). Importantly, in that previous study drug release was only monitored during 80 d. Relatively good agreement between theory and experiment had been observed. In the present study, the same *apparent* dexamethasone diffusion coefficient for this type of silicone, loaded with 10% drug, was used to predict the release patterns from the investigated electrode-free implants upon exposure to well agitated artificial perilymph at 37 °C: $D = 1.3 \times 10^{-13}$ cm^2/s. The black curves in the diagrams at the bottom of Fig. 4 show these theoretical predictions. The diagram on the right hand side is a zoom on the first 7 months and shows the experimentally measured release kinetics from 4 individual implants (error bars are too small to be visible). As it can be seen, the agreement between theoretical prediction (black curve) and independent experiments (symbols) is *rather* good, but there are clear and *systematic* deviations: At early time points, the theory overestimates drug release, at later time points, dexamethasone release is underestimated. This can probably be attributed to the fact that Eq. 1 is based on the assumption that the diffusion coefficient of the drug is *constant* over time and independent of the position in the implant. In reality, this is likely not the case for the following reason: Upon exposure to the release medium, drug crystals located in surface near regions can be expected to dissolve *first*. Once dissolved, the drug diffuses out. Consequently, water-filled "pores" are created. To a certain extend these "pores" might be partially closed by (even limited) swelling/expansion of surrounding silicone. In any case, it is likely that these zones in the silicone matrix become more permeable for the drug. Thus, dexamethasone, which subsequently diffuses from the center of the implants to the surface, can be expected to be more mobile in such drug-exhausted regions. Eq. 1 does not take this phenomenon into account. The apparent diffusion coefficient (being a measure for the mobility of the drug in the polymeric matrix) used in this equation presents a "*time-averaged*" value. It overestimates the real diffusion coefficient at early time points and underestimates drug mobility at late time points ("ignoring" the creation of "higher mobility regions" upon drug release). The diagram on the right hand side at the bottom of Fig. 4 nicely illustrates this initial

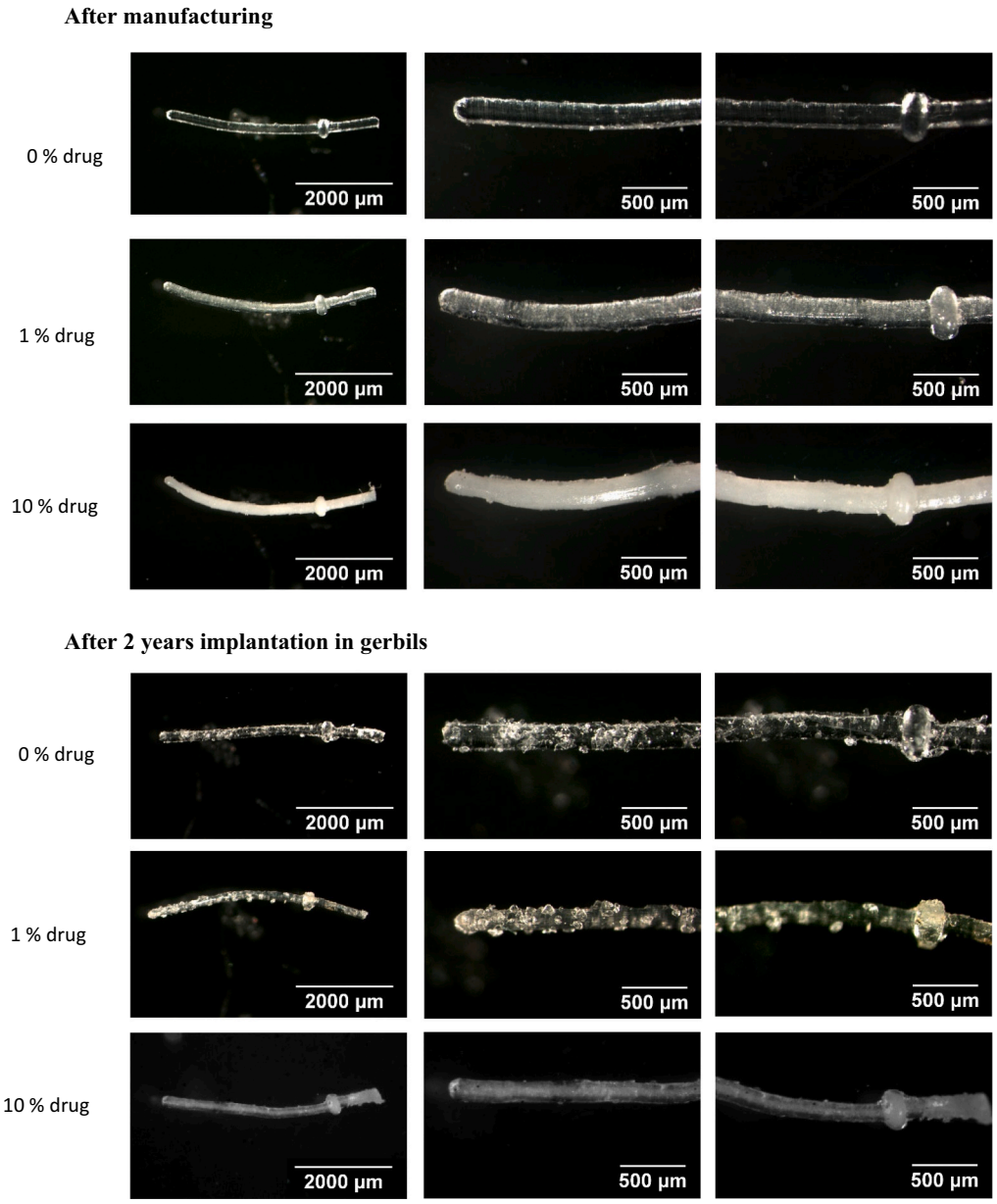

Fig. 10. Optical microscopy pictures of cochlear implants for gerbils before (top) implantation and after 2 years implantation in vivo (bottom). The initial dexamethasone loading was 0, 1 or 10% (as indicated on the left hand side). Please note that in the case of implants explanted after 2 years from gerbils, which were initially loaded with *10% drug*, particle deposits on the systems' surface had been removed before taking the picture (in contrast to the other samples).

overestimation and subsequent underestimation of drug release from the investigated cochlear implants. Please note that a more comprehensive mathematical theory, taking into account *time-dependent* diffusion coefficients (and ideally also *position-dependent* diffusivities), can be expected to be able to more reliably describe the observed drug release kinetics. However, the development of such a model was beyond the scope of this study.

The fact that the diffusion coefficient used for the above predictions was determined in *non-agitated* artificial perilymph likely only plays a minor role (if at all), since the effects of bulk fluid agitation on drug release were shown to be of negligible importance on dexamethasone release from thin films based on the same type of silicone (Krenzlin et al., 2012). Furthermore, the fact that *perfect sink conditions* were not always maintained in the surrounding bulk fluid in the present study might contribute to the observed deviations between theory and experiment (Fig. 4). However, the degree of drug saturation in the release medium rarely exceeded 30% (and very rarely 50%). Furthermore, high drug concentrations in the release medium were observed *occasionally* throughout the observation period (due to prolonged non-sampling periods during holidays or COVID lockdowns), whereas the under- and overestimation of drug release was *systematic*: overestimation at early time points, underestimation at later time points (Fig. 4).

3.3. Raman imaging: in vitro and ex vivo

Fig. 5 shows the Raman spectra of the investigated pure silicone (cochlear implants free of drug) and dexamethasone (powder as received). Importantly, the two spectra show multiple Raman bands at different frequencies. These differences can be used to distinguish between the two compounds and, thus, allow for Raman imaging of cross-sections of implants before and after exposure to artificial perilymph or implantation into gerbils.

A radial cross-section of a cochlear implant loaded with 10% dexamethasone (for use in humans, but free of metal electrodes) is shown in

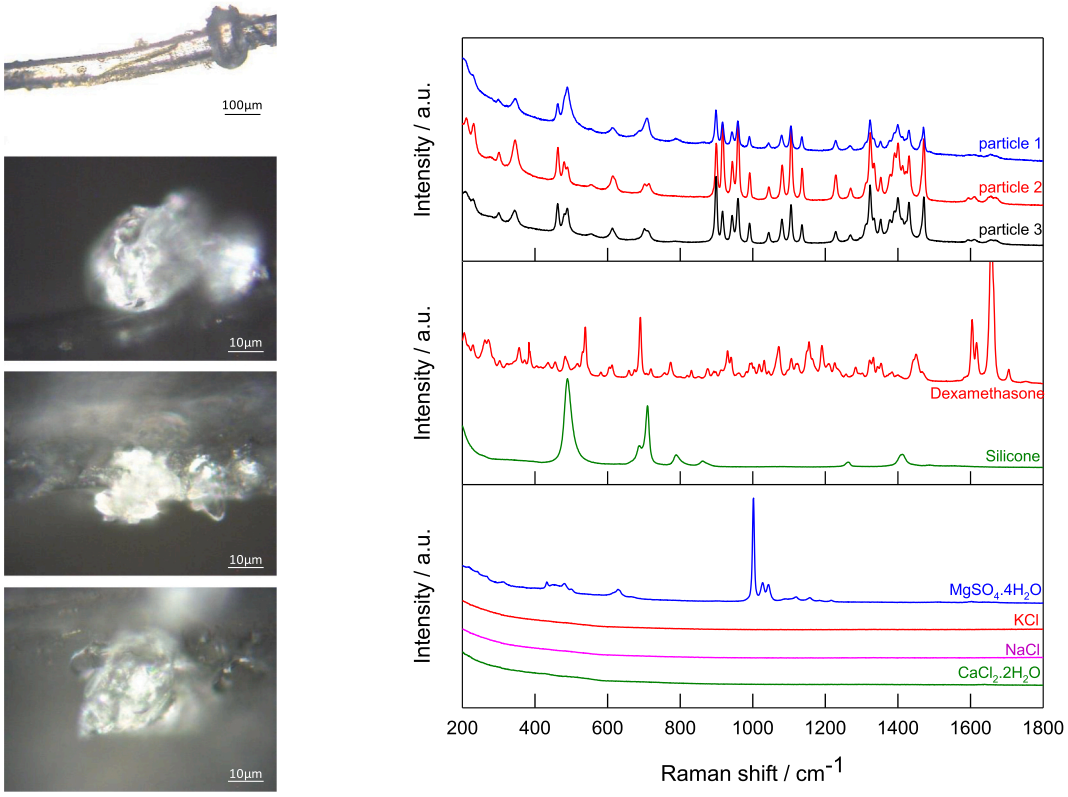

Fig. 11. *Left hand side:* Optical microscopy picture of a cochlear implant explanted from a gerbil after 2 years (top), and zooms on deposits observed at the implant's surface. *Right hand side:* Raman spectra of 3 particle deposits and different reference substances (as indicated).

Fig. 6 (before exposure to release media or implantation in vivo). From the left to the right, the following images can be seen: an optical microscopy picture, an image highlighting the silicone-rich regions in red, an image highlighting the dexamethasone-rich regions in green, and an overlap picture of the two (green and red being "false colors"). The cross-section was divided into small "pixels" and the Raman spectrum of each pixel was recorded. The relative importance of the contribution of dexamethasone and silicone was calculated, based on the reference spectra. Pixels rich in silicone are marked in red, pixels rich in dexamethasone are marked in green. So, please note that a red color does not strictly exclude the presence of *any* dexamethasone, nor does the green color strictly exclude the presence of *any* silicone. The penetration depth for these measurements was about 20–25 µm. As it can be seen in Fig. 6, the dexamethasone was indeed homogeneously distributed throughout the implant, confirming the hypothesis based on the optical microscopy above.

Fig. 7 shows an optical microscopy picture and Raman images of a radial cross-section of a cochlear implant *after 1 month exposure* to artificial perilymph at 37 °C in vitro. As it can be seen, dexamethasone-rich regions are still distributed *throughout* the implant, with a very few exceptions appearing in black close to the system's surface, which might indicate regions from which drug crystals have been released (highlighted by the white flashes). These pictures are in good agreement with the experimentally measured drug release kinetics (Fig. 4): After 1 month, only very minor amounts of drug are released. Furthermore, the Raman images are consistent with the hypothesized drug release mechanism: Water penetrating into the implants first reaches surface-near dexamethasone crystals, which dissolve and disappear.

To better understand the in vivo fate of this type of advanced drug delivery systems, dexamethasone-loaded cochlear implants were placed into gerbil ears and explanted after 2 years. Fig. 8 shows Raman images of an *axial* cross-section of an implant sample. The picture at the top on the left hand side shows the distribution of silicone. The picture in the middle illustrates the distribution of dexamethasone. The color scales indicate the relative concentrations of the compounds. The picture on the right hand side is an overlap: Silicone-rich regions are marked in red, dexamethasone-rich regions in green. Clearly, especially surface-near regions were virtually depleted of dexamethasone, while regions closer to the center of the implants still contained drug. This further confirms the hypothesis that drug diffusion is the dominant mass transport mechanism in this type of miniaturized implants (combined with limited drug solubility effects). The bottom row in Fig. 8 shows examples of Raman spectra recorded in silicone-rich and dexamethasone-rich pixels (the reference spectra of the two pure components are shown for reasons of comparison on the left hand side: red-silicone; green-dexamethasone). Fig. 9 shows Raman images of two *radial* cross-sections (obtained at different positions) of a cochlear implant, which was explanted from a gerbil after 2 years. The pictures at the top correspond to one cross-section, the pictures at the bottom to the other. The implant was initially loaded with 10% dexamethasone. Again, silicone-rich regions are marked in red, dexamethasone-rich regions in green. The picture on the right hand side at the top is an overlap image. Clearly, in the cross-section shown in the top row, a relatively large drug crystal (or an agglomerate of smaller dexamethasone crystals) can be seen. In contrast, in the cross-section shown in the bottom row, no comparable drug-rich regions are visible. This further confirms the hypothesis that the drug is initially homogeneously distributed throughout the cylindrical implants in the form of tiny dexamethasone crystals and that drug diffusion through the silicone matrix plays a major role. By chance, the images in the top row of Fig. 9 show a cross-section containing a dexamethasone crystal (or agglomerate of smaller crystals), which has (have) not yet been released after 2 years in vivo

implantation, whereas the pictures in the bottom row show a cross-section, from which virtually all drug has been released at this time point, or which never contained any drug (the initial drug loading was 10%).

3.4. Optical microscopy before and after 2 years implantation in gerbils

Fig. 10 shows optical microscopy pictures of cochlear implants for gerbils initially loaded with 0, 1 or 10% dexamethasone (as indicated). The images at the top were obtained before implantation, those at the bottom after 2 years implantation into the animals. As it can be seen, drug-free implants were transparent after manufacturing. The addition of increasing amounts of dexamethasone rendered the systems more and more opaque. This can be explained by the presence of dexamethasone in the form of tiny crystals in the silicone matrices, which are distributed throughout the devices. Importantly, the drug distribution is homogenous throughout the entire cochlear implants. In contrast, after 2 years implantation in gerbils, the systems have become transparent in surface-near regions, while the center of the devices remained opaque (bottom row of images in Fig. 10). This is a further confirmation of the above described, hypothesized drug release mechanism: Upon water penetration into the implants, first drug crystals located close to the systems' surface dissolve and disappear.

Interestingly, particle deposits were visible on the surface of all implants after 2 years implantation into gerbils, irrespective of the initial drug loading (please note that the deposits were removed prior to taking the pictures in the case of 10% drug loading, for the sake of visibility). These deposits might potentially be salts contained in the artificial perilymph, dexamethasone or stemming from the silicone matrix. To know whether this was the case, Raman spectra of these particle deposits were recorded. Optical microscopy pictures of such particle deposits are shown on the left hand side of Fig. 11. The Raman spectra are shown at the top on the right hand side of Fig. 11. Clearly, multiple peaks were visible in all 3 samples, at the same frequencies. Importantly, these peaks did not correspond to those observed in the spectra of the reference substances (dexamethasone, silicone, compounds of the artificial perilymph). Thus, the deposits formed in vivo have a different (biological) origin. It was beyond the scope of this study to analyze their composition in more detail.

4. Conclusion

Silicone-based cochlear implants for use in humans and animals (e.g., gerbils) can reliably control dexamethasone release over several years. Diffusional mass transport combined with drug saturation effects *within* the implants seem to play a major role. The drug is initially homogeneously distributed throughout the devices in the form of tiny dexamethasone crystals. Since the polymeric matrix is hydrophobic, only limited amounts of water can penetrate into the system and dissolve the dexamethasone particles only partially. With time, first surface-near regions become depleted of drug (in vitro as well as in vivo), as evidenced by optical microscopy and Raman imaging. Importantly, the implants do not swell or shrink to a noteworthy extent upon exposure to living tissue or artificial perilymph *for several years*. A simplified mathematical model can be used to predict the resulting drug release kinetics as a function of the implant's design. This can be very helpful for product optimization, in particular because the targeted release periods are very long and experimental feedback is only obtained very slowly.

Declaration of Competing Interest

The Editor-in-Chief of the journal is one of the co-authors of this article. The manuscript has been subject to all of the journal's usual procedures, including peer review, which has been handled independently of the Editor-in-Chief.

Data availability

Data will be made available on request.

Acknowledgements

This project has received funding from the French National Research Agency (ANR-15-CE19-0014-01/03) and from the Interreg 2 Seas programme 2014-2020 co-funded by the European Regional Development Fund under subsidy contract "Site Drug 2S07-033".

References

Aksit, A., Rastogi, S., Nadal, M.L., Parker, A.M., Lalwani, A.K., West, A.C., Kysar, J.W., 2021. Drug delivery device for the inner ear: ultra-sharp fully metallic microneedles. Drug Deliv. Transl. Res. 11, 214–226.

Astolfi, L., Simoni, E., Giarbini, N., Giordano, P., Pannella, M., Hatzopoulos, S., Martini, A., 2016. Cochlear implant and inflammation reaction: safety study of a new steroideluting electrode. Hear. Res. 336, 44–52.

Bas, E., Bohorquez, J., Goncalves, S., Perez, E., Dinh, C.T., Garnham, C., Hessler, R., Eshraghi, A.A., Van De Water, T.R., 2016. Electrode array-eluted dexamethasone protects against electrode insertion trauma induced hearing and hair cell losses, damage to neural elements, increases in impedance and fibrosis: a dose response study. Hear. Res. 337, 12–24.

Bawuah, P., Zeitler, J.A., 2021. Advances in terahertz time-domain spectroscopy of pharmaceutical solids: a review. TrAC Trends Anal. Chem. 139 (116272), 1–12.

Borden, R.C., Saunders, J.E., Berryhill, W.E., Krempl, G.A., Thompson, D.M., Queimado, L., 2011. Hyaluronic acid hydrogel sustains the delivery of dexamethasone across the round window membrane. Audiol. Neurotol. 16, 1–11.

Borgquist, P., Körner, A., Piculell, L., Larsson, A., Axelsson, A., 2006. A model for the drug release from a polymer matrix tablet—effects of swelling and dissolution. J. Control. Release 113, 216–225.

Chin, O.Y., Diaz, R.C., 2019. State-of-the-art methods in clinical intracochlear drug delivery. Curr. Opin. Otolaryngol. Head Neck Surg. 27, 381–386.

Crank, J., 1975. The Mathematics of Diffusion, 2nd Ed. Clarendon Press, Oxford.

Dai, J., Long, W., Liang, Z., Wen, L., Yang, F., Chen, G., 2018. A novel vehicle for local protein delivery to the inner ear: injectable and biodegradable thermosensitive hydrogel loaded with PLGA nanoparticles. Drug Dev. Ind. Pharm. 44, 89–98.

Douchement, D., Terranti, A., Lamblin, J., Salleron, J., Siepmann, F., Siepmann, J., Vincent, C., 2015. Dexamethasone eluting electrodes for cochlear implantation: effect on residual hearing. Cochlear Implants Int. 16, 195–200.

El Kechai, N., Agnely, F., Mamelle, E., Nguyen, Y., Ferrary, E., Bochot, A., 2015. Recent advances in local drug delivery to the inner ear. Int. J. Pharmaceut. 494, 83–101.

El Kechai, N., Mamelle, E., Nguyen, Y., Huang, N., Nicolas, V., Chaminade, P., Yen-Nicolay, S., Gueutin, C., Granger, B., Ferrary, E., Agnely, F., Bochot, A., 2016. Hyaluronic acid liposomal gel sustains delivery of a corticoid to the inner ear. J. Control. Release 226, 248–257.

Engleder, E., Honeder, C., Klobasa, J., Wirth, M., Arnoldner, C., Gabor, F., 2014. Preclinical evaluation of thermoreversible triamcinolone acetonide hydrogels for drug delivery to the inner ear. Int. J. Pharmaceut. 471, 297–302.

Farahmand Ghavi, F., Mirzadeh, H., Imani, M., Jolly, C., Farhadi, M., 2010. Corticosteroid releasing cochlear implant: a novel hybrid of biomaterial and drug delivery system. J. Biomed. Mater. Res. 94B, 388–398.

Farhadi, M., Jalessi, M., Salehian, P., Ghavi, F.F., Emamjomeh, H., Mirzadeh, H., Imani, M., Jolly, C., 2013. Dexamethasone eluting cochlear implant: histological study in animal model. Cochlear Implants Int. 14, 45–50.

Forouzandeh, F., Zhu, X., Alfadhel, A., Ding, B., Walton, J.P., Cormier, D., Frisina, R.D., Borkholder, D.A., 2019. A nanoliter resolution implantable micropump for murine inner ear drug delivery. J. Control. Release 298, 27–37.

Gao, Z., Schwieger, J., Matin-Mann, F., Behrens, P., Lenarz, T., Scheper, V., 2021. Dexamethasone for inner ear therapy: biocompatibility and bio-efficacy of different dexamethasone formulations in vitro. Biomolecules 11, 1–14. https://doi.org/10.3390/biom11121896.

Gausterer, J.C., Saidov, N., Ahmadi, N., Zhu, C., Wirth, M., Reznicek, G., Arnoldner, C., Gabor, F., Honeder, C., 2020. Intratympanic application of poloxamer 407 hydrogels results in sustained N-acetylcysteine delivery to the inner ear. Eur. Pharm. Biopharm. 150, 143–155.

Hao, J., Li, S.K., 2019. Inner ear drug delivery: recent advances, challenges, and perspective. Eur. J. Pharm. Sci. 126, 82–92.

Jaudoin, C., Agnely, F., Nguyen, Y., Ferrary, E., Bochot, A., 2021a. Nanocarriers for drug delivery to the inner ear: physicochemical key parameters, biodistribution, safety and efficacy. Int. J. Pharmaceut. 592 (120038), 1–31.

Jaudoin, C., Carree, F., Gehrke, M., Sogaldi, A., Steinmetz, V., Hue, N., Cailleau, C., Tourrel, G., Nguyen, Y., Ferrary, E., Agnely, F., Bochot, A., 2021b. Transtympanic injection of a liposomal gel loaded with N-acetyl-L-cysteine: a relevant strategy to prevent damage induced by cochlear implantation in guinea pigs? Int. J. Pharmaceut. 604 (120757), 1–14.

Jia, H., François, F., Bourien, J., Eybalin, M., Lloyd, R.V., Van De Water, T.R., Puel, J.L., Venail, F., 2016. Prevention of trauma-induced cochlear fibrosis using intracochlear application of anti-inflammatory and antiproliferative drugs. Neuroscience 316, 261–278.

Krenzlin, S., Vincent, C., Munzke, L., Gnansia, D., Siepmann, J., Siepmann, F., 2012. Predictability of drug release from cochlear implants. J. Control. Release 159, 60–68.
Lao, L.L., Venkatraman, S.S., Peppas, N.A., 2008. Modeling of drug release from biodegradable polymer blends. Eur. J. Pharm. Biopharm. 70, 796–803.
Lehner, E., Guendel, D., Liebau, A., Plontke, S., Maeder, K., 2019. Intracochlear PLGA based implants for dexamethasone release: challenges and solutions. Int. J. Pharmaceut. X 1 (100015), 1–9.
Lehner, E., Liebau, A., Syrowatka, F., Knolle, W., Plontke, S.K., Maeder, K., 2021. Novel biodegradable round window disks for inner ear delivery of dexamethasone. Int. J. Pharmaceut. 594 (120180), 1–9.
Lehner, E., Menzel, M., Guendel, D., Plontke, S.K., Maeder, K., Klehm, J., Kielstein, H., Liebau, A., 2022. Microimaging of a novel intracochlear drug delivery device in combination with cochlear implants in the human inner ear. Drug Deliv. Transl. Res. https://doi.org/10.1007/s13346-021-00914-9, 257-266.
Liu, Y., Jolly, C., Braun, S., Janssen, T., Scherer, E., Steinhoff, J., Ebenhoch, H., Lohner, A., Stark, T., Kiefer, J., 2015. Effects of a dexamethasone-releasing implant on cochleae: a functional, morphological and pharmacokinetic study. Hear. Res. 327, 89–101.
Liu, Y., Jolly, C., Braun, S., Stark, T., Schere, E., Plontke, S.K., Kiefer, J., 2016. In vitro and in vivo pharmacokinetic study of a dexamethasone-releasing silicone for cochlear implants. Eur. Arch. Otorhinolaryngol. 273, 1745–1753.
Maeder, K., Lehner, E., Liebau, A., Plontke, S.K., 2018. Controlled drug release to the inner ear: Concepts, materials, mechanisms, and performance. Hear. Res. 368, 49–66.
McCoy, C.F., Spence, P., Dallal Bashi, Y.H., Murphy, D.J., Boyd, P., Dangi, B., Derrick, T., Devlin, B., Kleinbeck, K., Malcolm, R.K., 2021. Use of simulated vaginal and menstrual fluids to model in vivo discolouration of silicone elastomer vaginal rings. Int. J. Pharmaceut. X 3 (100081), 1–10.
Mond, H.G., Stokes, K.B., 1996. The steroid-eluting electrode: a 10-year experience. Pace 19, 1016–1020.
Nordvik, O., Laugen Heggdal, P.O., Brännström, J., Vassbotn, F., Aarstad, A.K., Aarstad, H.J., 2018. Generic quality of life in persons with hearing loss: a systematic literature review. BMC Ear Nose Throat Disord. 18 (1), 1–13.
Oliveira, P., Willart, J.F., Siepmann, J., Siepmann, F., Descamps, M., 2018. Using milling to explore physical states: the amorphous and polymorphic forms of dexamethasone. Cryst. Growth Des. 18, 1748–1757.
Olusanya, B.O., Neumann, K.J., Saunders, J.E., 2014. The global burden of disabling hearing impairment: a call to action. Bull. World Health Organ. 92, 367–373.
Palugan, L., Cerea, M., Cirilli, M., Moutaharrik, S., Maroni, A., Zema, L., Melocchi, A., Uboldi, M., Filippin, I., Foppoli, A., Gazzaniga, A., 2021. Intravesical drug delivery approaches for improved therapy of urinary bladder diseases. Int. J. Pharmaceut. X 3 (100100), 1–11.
Punčochová, K., Vukosavljevic, B., Hanuš, J., Beránek, J., Windbergs, M., Štěpánek, F., 2016. Non-invasive insight into the release mechanisms of a poorly soluble drug from amorphous solid dispersions by confocal Raman microscopy. Eur. J. Pharm. Biopharm. 101, 119–125.
Qnouch, A., Solarczyk, V., Verin, J., Tourrel, G., Stahl, P., Danede, F., Willart, J.F., Lemesre, P.E., Vincent, C., Siepmann, J., Siepmann, F., 2021. Dexamethasone-loaded cochlear implants: how to provide a desired "burst release". Int. J. Pharmaceut. X 3 (100088), 1–10.
Siepmann, J., Siepmann, F., 2013. Mathematical modeling of drug dissolution. Int. J. Pharmaceut. 453, 12–24.
Siepmann, J., Siepmann, F., 2020. Sink conditions do not guarantee the absence of saturation effects. Int. J. Pharmaceut. 577 (119009), 1–11.
Swan, E.E., Mescher, M., Sewell, W., Tao, S., Borenstein, J., 2008. Inner ear drug delivery for auditory applications. Adv. Drug Deliv. Rev. 60, 1583–1599.
Toulemonde, P., Risoud, M., Lemesre, P.E., Beck, C., Wattelet, J., Tardivel, M., Siepmann, J., Vincent, C., 2021. Evaluation of the efficacy of dexamethasone-eluting electrode 2 array on the post-implant cochlear fibrotic reaction by three-3 dimensional immunofluorescence analysis in Mongolian gerbil 4 cochlea. J. Clin. Med. 10 (3315), 1–13.
Vukosavljevic, B., De Kinder, L., Siepmann, J., Muschert, S., Windbergs, M., 2016. Novel insights into controlled drug release from coated pellets by confocal Raman microscopy. J. Raman Spectrosc. 47, 757–762.
World Health Organization, 2021. World report on hearing, ISBN 978–92–4-002048-1. https://www.who.int/teams/noncommunicable-diseases/sensory-functions-disability-and-rehabilitation/highlighting-priorities-for-ear-and-hearing-care.
Zeitler, J.A., Shen, Y., Baker, C., Taday, P.F., Pepper, M., Rades, T., 2007. Analysis of coating structures and interfaces in solid oral dosage forms by three dimensional terahertz pulsed imaging. J. Pharm. Sci. 96, 330–340.